Bioresource Technology 434 (2025) 132787

Contents lists available at ScienceDirect

Bioresource Technology

journal homepage: www.elsevier.com/locate/biortech

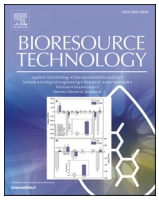

Effects of feeding strategy on cathodic electro-fermentation of xylose with mixed microbial cultures

Yu Sun [a], Antti J. Rissanen [a,b], Gaia Salvatori [c], Marianna Villano [c], Marika Kokko [a,*]

[a] Faculty of Engineering and Natural Sciences, Tampere University, Korkeakoulunkatu 8, 33720 Tampere, Finland
[b] Natural Resources Institute Finland, Latokartanonkaari 9, 00790 Helsinki, Finland
[c] Department of Chemistry, Sapienza University of Rome, P.le Aldo Moro 5, 00185 Rome, Italy

HIGHLIGHTS

- Repeated batch and continuous feeding strategies were compared using mixed cultures.
- Repeated batch CEF favored propionate and butyrate production.
- CEF achieved 2.5 × higher propionate production rates than the control.
- *Clostridium* genera played a pivotal role in xylose CEF.

GRAPHICAL ABSTRACT

Created with BioRender.com/vnv7gsz

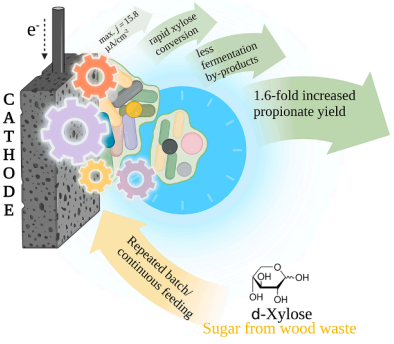

ARTICLE INFO

Keywords:
Cathodic electro-fermentation
Xylose
Carboxylic acids
Digested sewage sludge
Selection pressure

ABSTRACT

Xylose fermentation is sometimes hindered by unbalanced redox states, limiting its efficiency in industrial biotechnology applications. Recent advancements in cathodic electro-fermentation (CEF) technologies have addressed this issue by regulating the metabolic states of microorganisms and modulating intercellular electron transfer using a cathode electrode. However, the feasibility of mixed culture CEF using xylose as the feedstock has not been studied. This study investigated feeding strategies in mixed culture CEF systems to enhance the production rates and yields of carboxylic acids, namely propionate and butyrate, using xylose as the substrate over runs lasting ca. 25 days. The results compared the repeated batch and continuous cathodic electro-fermentation systems (poised cathode potential −0.40 V vs. standard hydrogen electrode) and analyzed their microbial community compositions. The repeated batch CEF systems demonstrated rapid and consistent steered metabolism towards propionate and butyrate, achieving higher yields for propionate (1.57-fold) and butyrate (1.64-fold) compared to the open-circuit controls. In contrast, continuous systems did not exhibit cathode-assisted metabolism. The microbial community analyses suggested that *Clostridium,* in both biofilm and planktonic cells, played a pivotal role in cathodic xylose electro-fermentation. These findings highlight the potential of repeated batch CEF systems for enhancing carboxylic acid production.

* Corresponding author.
E-mail address: marika.kokko@tuni.fi (M. Kokko).

https://doi.org/10.1016/j.biortech.2025.132787
Received 7 March 2025; Received in revised form 30 May 2025; Accepted 7 June 2025
Available online 8 June 2025

1. Background

The expansion of the agriculture and forestry industry generated approximately 2.5 million tonnes of waste (CO_2-eq) in 2021 (FAO-UN, 2021). Conventional methods for waste management in these fields, e.g., physical, chemical, and biological processes, need up-to-date technological advancements to integrate with circular economy practices (Demirbas, 2011). For example, lignocellulosic material recovered from forest industry waste has shown broad applications in industrial biorefineries for food additives and biochemical productions (Nanda et al., 2015; Ponnusamy et al., 2019). Modern fermentation technology plays a key role in many industrial biorefineries, featuring microorganisms forming oxidized and reduced compounds by achieving their metabolic balances under energy-controlled conditions (Moscoviz et al., 2018; Octave and Thomas, 2009; Trchounian and Trchounian, 2019).

D-xylose ($C_5H_{10}O_5$), a sugar obtained from lignocellulosic waste, can serve as a valuable raw material for fermentation processes. Xylose fermentation is an environment-friendly approach for biorefining value-added chemicals, e.g., ethanol, 1,4-butanediol, 1,2,4-butanetriol, ethylene glycol, glycolate, xylitol, and succinate (Cirino et al., 2006; Liu et al., 2012; Zhang et al., 2016a; Zhang et al., 2016b; Zhao et al., 2020). However, pure culture xylose fermentation is frequently constrained by unbalanced metabolic redox states primarily due to lower energy yields (e.g., ATP) compared to glucose fermentation. Many bacterial candidates require genetic modifications to enable or enhance xylose uptake and utilisation, limiting their practical application in industrial processes (Domingues et al., 2021; Gu et al., 2010; Jeffries, 1983; Zhao et al., 2020). Both native and engineered cultures for xylose fermentation have encountered bottlenecks such as by-product accumulation and increased susceptibility to environmental stressors (Guan et al., 2017). Alternatively, mixed culture xylose fermentation has been explored, offering robustness, energy conservation, and cost-effective solutions for the sustainable production of biofuels and biochemicals (Khedkar et al., 2024; Temudo et al., 2009).

In mixed culture fermentation, dynamic metabolic redox states and complex interspecies relations lead to a diverse spectrum of metabolic products, e.g., organic acids (e.g., acetate, propionate, butyrate, lactate, succinate, and caproate) and solvents (e.g., ethanol, butanol, and acetone) (Dai et al., 2017). One innovative approach to enhance production yields and titers of the desired products in conventional mixed culture fermentation is to use cathodic electro-fermentation (CEF) systems (Moscoviz et al., 2016; Schievano et al., 2016; Vassilev et al., 2021; Virdis et al., 2022). In CEF, the cathode electrode has been suggested to assist in controlling the extracellular oxidation–reduction potential (ORP) in the fermentation broth or serves as an electron donor to steer the microbial metabolism towards the production of cellular reducing equivalents (Moscoviz et al., 2016; Virdis et al., 2022).

Many mixed culture CEF studies have focused on enhancing glucose fermentation due to its rapid ATP generation, high metabolic rates, and wide range of metabolic end products produced by various microorganisms. For example, glucose-fed mixed culture CEF notably enhanced production share of butyrate by approximately 1.57-fold, and ethanol by 1.8-fold, compared to open circuit voltage (OCV) conditions (Toledo-Alarcón et al., 2019). Similarly, *n*-butyrate production was enhanced by almost 8-fold when using neutral red as a mediator in glucose-fed mixed culture CEF (Paiano et al., 2019). Additionally, acetate also exhibited responses to the cathode, with 55 % enhanced production under the cathodic potential of −0.8 V vs. standard hydrogen electrode (SHE, Jiang et al., 2018). On the other hand, for xylose, the second most abundant sugar after glucose, its potential in mixed culture electro-fermentation (EF) systems remains unexplored. Studies revealed that xylose-fed CEF with *Clostridium autoethanogenum* redirected the metabolic pathways towards acetate and ethanol (Martínez-Ruano et al., 2024). As a state-of-the-art approach for optimizing mixed culture xylose fermentation, CEF offers improved control over metabolic pathways and enhances the production of valuable biochemicals.

A large fraction of CEF studies have been conducted in batch-operated systems with simplified reactor configurations. Nevertheless, batch-operated mixed culture CEF systems face several challenges, including nutrient depletion, end-product inhibition, limited control of biomass growth over long-term operation and restricted scalability (Cinar et al., 2003). Advanced feeding strategies, i.e., repeated batch and continuous feeding, can provide better pH control and prevent nutrient depletion and by-product inhibition (Cinar et al., 2003; Lee et al., 1999; Li et al., 2014). Studies related to non-hydrogen-driven mixed culture CEF systems operated under repeated substrate feeding cycles have reported that the poised cathodic potential enhanced butyrate production during the second feeding cycle (Paiano et al., 2019) and enhanced hydrogen and methane production for approximately 70 days with 15 feeding cycles with cathode potential adjusted to −0.80 V vs. SHE (Jiang et al., 2018). However, limited data is available to determine whether the poised cathodic potential can steer the production of carboxylic acids under repeated batch or continuous feeding. Therefore, investigating CEF systems operated under repeated batch and continuous xylose feeding schemes enables precise monitoring of cathode-assisted metabolism. Such evaluations are crucial for scaling up and advancing sustainable industrial biochemical processes.

This study investigated the potential of xylose-based carboxylic acids fermentation processes in mixed culture CEF systems for enhancing propionate and butyrate production. The potential application of CEF systems with the repeated batch and the continuous operation modes for uninterrupted steered propionate and butyrate production was evaluated. Furthermore, microbial community compositions in both planktonic and biofilm samples were characterized, and prospective integration of mixed culture CEF systems with optimized feeding strategies was discussed, providing a roadmap for enhancing product yields for the green chemicals production.

2. Materials and methods

2.1. Inoculum

Digested municipal sewage sludge, collected from the Viinikanlahti wastewater treatment plant (Tampere, Finland) was stored at 4 °C and used as the inoculum for all the experiments. Before initiating the electro-fermentation process, 5 mL (1.6 %, v/v) and 20 mL (6.3 %, v/v) of the sewage sludge was added to repeated batch and continuous experiments, respectively.

2.2. Bioelectrochemical reactor setup

The bioelectrochemical experiments were conducted using 300 mL H-type borosilicate reactors (Adams and Chittenden Scientific Glass, USA) and a three-electrode setup akin to the previous study (Sun et al., 2023). In brief, the cathode (working electrode) and anode (counter electrode) were made of carbon felt (17.9 cm^2 projected surface area, 1.1 cm thickness, Alfa Aesar, USA) wrapped around a graphite rod (15 cm × 3 mm, Sigma Aldrich, USA) and a platinum wire (10 cm × 0.4 mm, Advent Research Material Ltd, UK), respectively. A cation exchange membrane (19.6 cm^2 projected surface area, CMI-7000, Membranes International Inc. USA) was placed between the anodic and the cathodic chambers. A multichannel potentiostat (VMP3, BioLogic, France) was used to record the open-circuit voltage or to set the cathode potential to −0.60 V against an Ag/AgCl KCl_{sat} reference electrode (Xylem Analytics, Germany), corresponding to −0.40 V relative to the SHE, based on a previous mediator-less CEF study (Engel et al., 2019). All the potentials are herein reported vs. SHE (−0.197 V vs. Ag/AgCl KCl_{sat}). The OCV was set to record every 0.01 V potential change (dE_R, E_{range} = -10 V; 10 V) with 60-second intervals (dt_R). The cathodic chamber was sealed with generic acrylic glass (Ø 30 mm, 3 mm thickness) for repeated batch control experiments and otherwise shared the same configuration as the cathodic chamber in bioelectrochemical reactors (Fig. S1).

An aqueous phosphate buffer solution was used as the anolyte and contained (g/L): K_2HPO_4 (10.1), KH_2PO_4 (3.7), and NH_4Cl (3.0). The fermentation broth (catholyte) contained K_2HPO_4 (10.1), KH_2PO_4 (3.7), NH_4Cl (3.0), xylose (1.5–5.0), yeast extract (1.0), sodium 2-bromoethanesulfonate (2.1), $MgSO_4{\cdot}7H_2O$ (0.02), $CaCl_2$(0.015), 1.0 mL of vitamin solution and 10.0 mL of trace elements solution (Table S1; Table S2).

2.3. Bioelectrochemical reactor operation

Repeated batch and continuous systems were tested during the experiments. Table 1 shows the key parameters of reactors with two feeding modes used in this study. During operation, anaerobic conditions in the cathodic chamber were maintained by continuously purging the medium with N_2 gas with ca. 10 mL/min through a peristaltic tube (L/S 16, Masterflex, USA). Liquid samples were taken three times per week (repeated batch) or daily (continuous) from the cathodic chambers of the reactor. In repeated batch systems, 100 mL of catholyte was manually removed with 50 mL syringes at each sampling point. For continuous systems, the fresh medium was fed to the cathodic chamber after 14.3 h from start-up using peristaltic pumps (Ismatec ISM834C Reglo Digital, VWR, USA) at a 0.20 mL/min flow rate. The effluent of the continuous system was collected and weighed regularly to verify the hydraulic retention time (HRT).

2.4. Cyclic voltammetry

Cyclic voltammetry (CV) was performed as a separate experiment with the same three-electrode setup to characterize the electrode material. The cathodic and anodic chambers of the H-type reactors were filled with the same fermentation broth and phosphate buffer solutions, respectively, and used for all experiments. Current profiles were recorded by scanning the cathode potential at a scan rate of 0.10 mV/s within a potential window from 0.20 to −0.90 V vs. SHE to measure oxidation and reduction reactions of the solution. During the measurements, the temperature was controlled at 35 °C and stirring was switched off. Three cycles (repeats) were recorded at each CV measurement.

2.5. Analyses and calculations

The pH was measured using a pH meter (3110, WTW, Germany) and adjusted to 6.3 ± 0.1 using 1 M NaOH at each sampling point. Cell density was analyzed photometrically using a spectrophotometer (UV-1800, Shimadzu, Japan) with absorbance at 600 nm wavelength. Samples were filtered through 0.2 μm syringe filters (CHROMAFIL® Xtra PET-45/25, Germany) for the analysis of xylose, carboxylic acids, and alcohols. The concentrations of xylose were determined using high-performance liquid chromatography (HPLC SIL-20, Shimadzu, Japan) equipped with a refractive index (RI) detector and a sugar column (Rezex™ RHM-Monosaccharide H^+, 300 × 7.80 mm) operated under the following conditions: column temperature of 40 °C, injection volume of 15 μL, 10 mM sulfuric acid mobile phase at 0.50 mL/min flow rate with 30 min retention time. Concentrations of carboxylic acids and alcohols (acetate, ethanol, propionate, butyrate, isobutyrate, caproate) were determined using gas chromatography (Shimadzu GC-2010) with a column (Zebron ZB-WAX Plus, Phenomenex, USA), a flame ionization detector (FID) and helium as a carrier gas operated under the following conditions: flow rate of 84.4 mL/min, injector and detector temperatures of 250 °C, and the column temperature was first kept at 40 °C for 2 min, increased to 160 °C min at a rate of 20 °C/min, and further increased to 220 °C with a rate of 40 °C/min.

Table 1
Parameters tested in the repeated batch and continuous BES reactors.

Operation mode	Run time (d)	Starting xylose concentration (g/L)	Feeding strategy	HRT (d)	Organic loading rate (g/L/d)
Repeated batch	25.6	5	Replaced 100 mL 3 times per week	7.5 d	0.4
Continuous	8.9	1.5	Continuous feeding at 0.2 mL/min	1.1 d	1.4

The electrons transferred from the cathode during the electro-fermentation were calculated using a method similar to that described previously (Sun et al., 2023), i.e., the recorded current at each time point was multiplied by the time difference to the previous point (1 $A\ s = 1$ Coulomb (C)) and Faraday constant (96485.33 C/mol) was introduced to convert the value into mol electrons. Data of all time points were added to give the total mol of electrons, and the xylose concentrations plus the reactor volume were considered during the calculations. The average current densities were calculated based on total charge transferred ($Q\text{-}Q_0$) divided by electrode's projected surface area (17.9 cm^2) and operation time. The yield coefficients of quantified products were determined as the slope of plots of mol product versus total mol xylose consumed. The carbon balance (CB) was calculated for each measuring point using the equation below:

$$CB(\%) = \frac{[\sum_i (m_i \bullet n_i)_t]}{[\sum_i (m_i \bullet n_i)_{t_0}]} \times 100$$

where m_i is the absolute amount (mmol) of compound i at a specific time t; n_i is the number of carbon atoms of compound i. Time t_0 denotes the point of inoculation. The redox balance (RB) was calculated for each measuring point using the equation below:

$$RB(\%) = \frac{[\sum_i (m_i \bullet n_i \bullet \gamma)_t + e_{cathode}(t)]}{[\sum_i (m_i \bullet n_i \bullet \gamma)_{t_0} + e_{cathode}(t_0)]} \times 100$$

where $e_{cathode}(t)$ is the mmol of electrons donated by the cathode at specific time t and t_0 initial 0 h. The degree of reduction (γ) of the respective chemical with the elemental composition $C_aH_bO_cN_d$ was calculated based on the equation below:

$$\gamma = \frac{a \times 4 + b \times 1 + c \times (-2) + d \times (-3)}{a}$$

The carbon and redox balance calculations did not consider any biomass and gas production (e.g., CO_2 and H_2) due to the continuous N_2 sparging in all systems.

2.6. Characterization of the microbiome

Planktonic cells and biofilm samples were collected from the cathodic chamber, including 40 mL of fermentation broth of the repeated batch reactor after 165 h and 641 h, 40 mL of fermentation broth and biofilm sample from the cathode electrode of the continuous experiment after 213 h. The electrode material samples were soaked in 35 mL of phosphate buffer solution and ultrasonicated for 15 min (USC 300 T, VWR, USA). The planktonic cells and biofilm samples were centrifuged (8000 rpm, 10 min) to remove the supernatant, and the pellets were resuspended in 1 mL of the phosphate buffer solution. The samples were stored at −80 ℃ and thawed at room temperature before the DNA extraction. The DNA extraction was performed using the DNeasy PowerSoil Pro Kit (Qiagen, Germany) in accordance with the manufacturer's protocol, and the DNA concentrations were measured using a spectrophotometer (NanoDrop™ 1000, Thermo Fisher Scientific, USA).

The DNA samples were sequenced using the Illumina NovaSeq PE250 platform (Illumina, USA) at a depth of 50 K reads (Biomarker Technologies, Germany). For sequencing, the V3–V4 region of the 16S rRNA gene was PCR-amplified using the primer pair 341F/806R (5′-3′ sequence: ACTCCTACGGGAGGCAGCA / GGACTACHVGGGTWTCTAAT). The basic bioinformatic analyses were done by Biomarker

Technologies (Germany), including raw read trimming using Trimmomatic (v0.33) (Bolger et al., 2014), primer sequence removal using Cutadapt (v1.9.1) (Martin, 2011), paired-end read assembly using Usearch (v10) (Edgar, 2010), chimeric sequence removal using UCHIME (Edgar et al., 2011), and sequence denoising to generate amplicon sequence variants (ASV) using the DADA2 method (Callahan et al., 2016) in QIIME2 (Bolyen et al., 2019). Taxonomic annotation of the ASVs was conducted using the Naive Bayes classifier-based method (classify-sklearn in QIIME) against Silva 138 database (Quast et al., 2013). Coverage ranged from 0.999 to 1 in each library, confirming that sequence variation was adequately covered. Beta-diversity differences (Bray-Curtis dissimilarity metric) among samples were visualised using non-metric multidimensional scaling (NMDS) analyses, conducted using PAST (v4.02) (Hammer et al., 2001), and the 95 % confidence ellipses were calculated using error-ellipse package in MATLAB (Johnson, 2024). The results were tested between treatment groups using permutational analysis of variance (PERMANOVA) using the adonis function in the vegan package in R (Anderson, 2017; Oksanen et al., 2001). The 16S rRNA gene amplicon sequencing reads generated in this study have been deposited in the European Nucleotide Archive (ENA) under the project accession number ERP163316.

3. Results and discussion

3.1. Cathode-assisted propionate and butyrate production in repeated batch system

Repeated batch systems were tested to investigate the end-product spectrum of the xylose-fed CEF process. During the initial batch stage from 0 to 41 h, all reactors showed rapid anaerobic planktonic cell growth ($OD_{AP} = 0.9 \pm 0.1$ vs. $OD_{control} = 1.1 \pm 0.2$, compared to initial OD = 0.1, Fig. 1), accompanied by prompt xylose depletion (Fig. S2) and noticeable biomass growth on the cathode material (visual observation, figure not shown). Many anaerobes that grow on xylose have lower

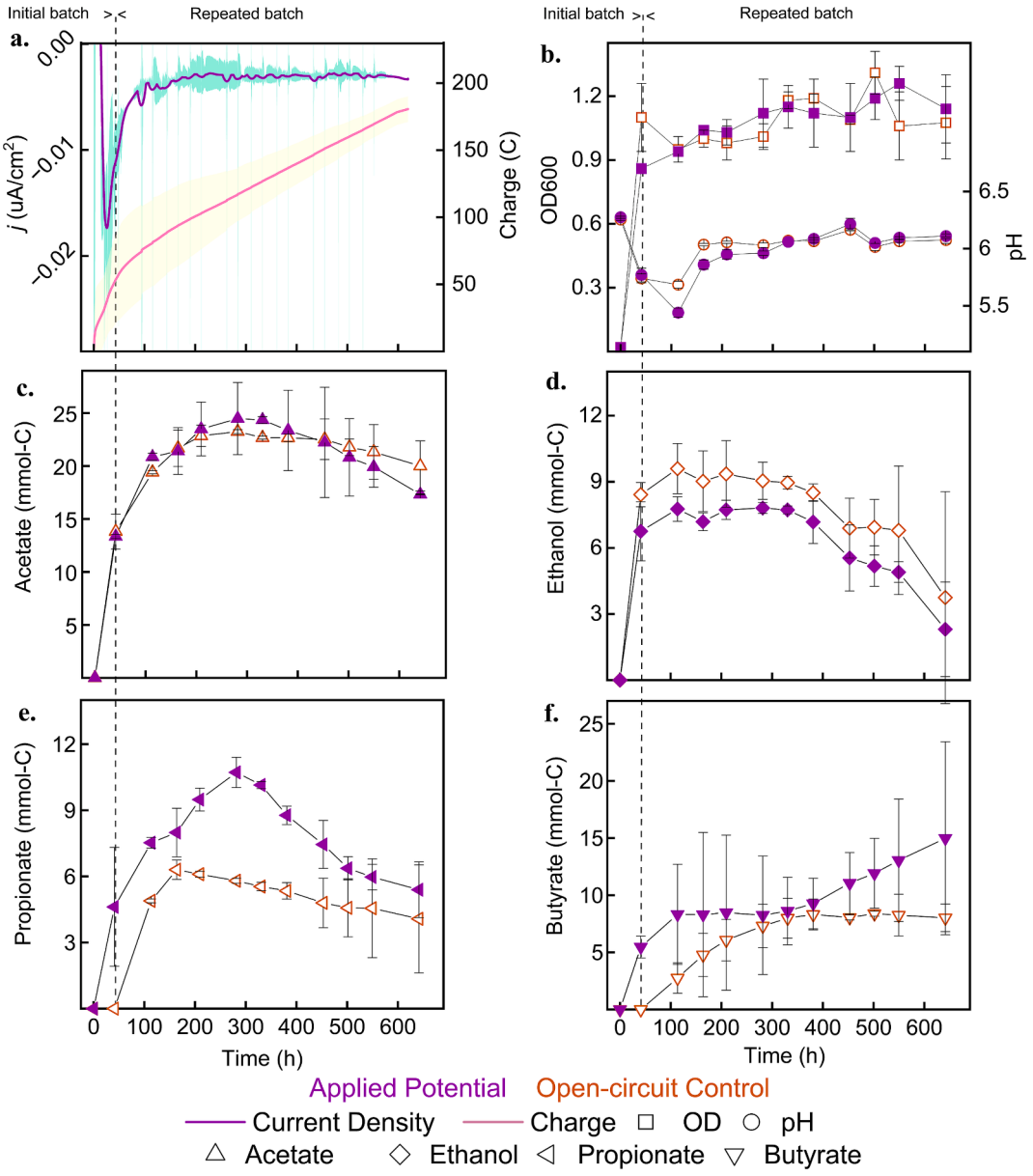

Fig. 1. Mixed culture repeated batch electro-fermentation using xylose as substrate. Current density and charge logged at a poised cathode potential of −0.40 V (a), OD and pH (b), and the accumulated amount of acetate, ethanol, propionate, and butyrate (c-f) measured from the reactor with applied potential (AP) and open-circuit reactors (control). The dashed lines denote the time when the media replacement begins. Xylose concentrations can be found in the supplementary file (Fig. S2). All repeated batch results were based on the average data of two biological replicates, and ranges were represented as error bars.

biomass yields than other carbon sources, e.g., glucose (Temudo et al., 2009). The drop in current density (from 0 to −0.017 μA/cm^2) in the AP reactors (Fig. 1) and similar OD measured in the AP and control reactors indicated that the cathode served as an additional energy source for xylose catabolism without significantly affecting the planktonic cell growth during the initial batch period. Meanwhile, the pH dropped from 6.3 to 5.8 in the AP (i.e., applied potential) and control reactors (Fig. 1). Acetate and ethanol were produced in all reactors (Fig. S3) whereas propionate and butyrate were only produced in the AP reactors during this period (Fig. 1). Other potential intermediate products, e.g., lactate and formate (Kongjan et al., 2009; Temudo et al., 2009), were not detected during the experiments.

The initial batch period results highlighted the early cathode-assisted production of propionate (4.61 ± 2.70 mmol-C, AP vs. 0 mmol-C, control) and butyrate (5.47 ± 0.96 mmol-C, AP vs. 0 mmol-C, control). Although propionate and butyrate production is sometimes observed during traditional xylose fermentation (Qian et al., 2020; Tang et al., 2022), the simultaneously enhanced propionate and butyrate production by mixed culture cathode-assisted EF systems has not been reported before. Thus, the results indicated that the cathode exerted notable influences on the formation of products with a higher degree of reduction equivalents (Kracke and Krömer, 2014), e.g., propionate, butyrate, and ethanol, as opposed to acetate that was produced at similar amounts in all reactors during the batch stage.

After 41 h, the repeated batch operation started (HRT = 7.5 d). During this period, the trend in AP reactors continued with higher propionate and butyrate concentrations measured than in the controls. By the end of the repeated batch operation, a 1.57-fold higher propionate and 1.64-fold higher butyrate yields were observed in AP reactors with the highest propionate production rate of 4.4 ± 0.4 mg/L/h (vs. 1.8 ± 0.1 mg/L/h, control), propionate yield of 0.09 ± 0.5 $mol_{product}/mol_{xylose}$ (vs. 0.06 ± 0.01 $mol_{product}/mol_{xylose}$, control). The control reactors showed marginally higher ethanol yields of 0.13 ± 0.01 $mol_{product}/mol_{xylose}$, (vs. 0.10 ± 0.01 $mol_{product}/mol_{xylose}$, AP), while the acetate

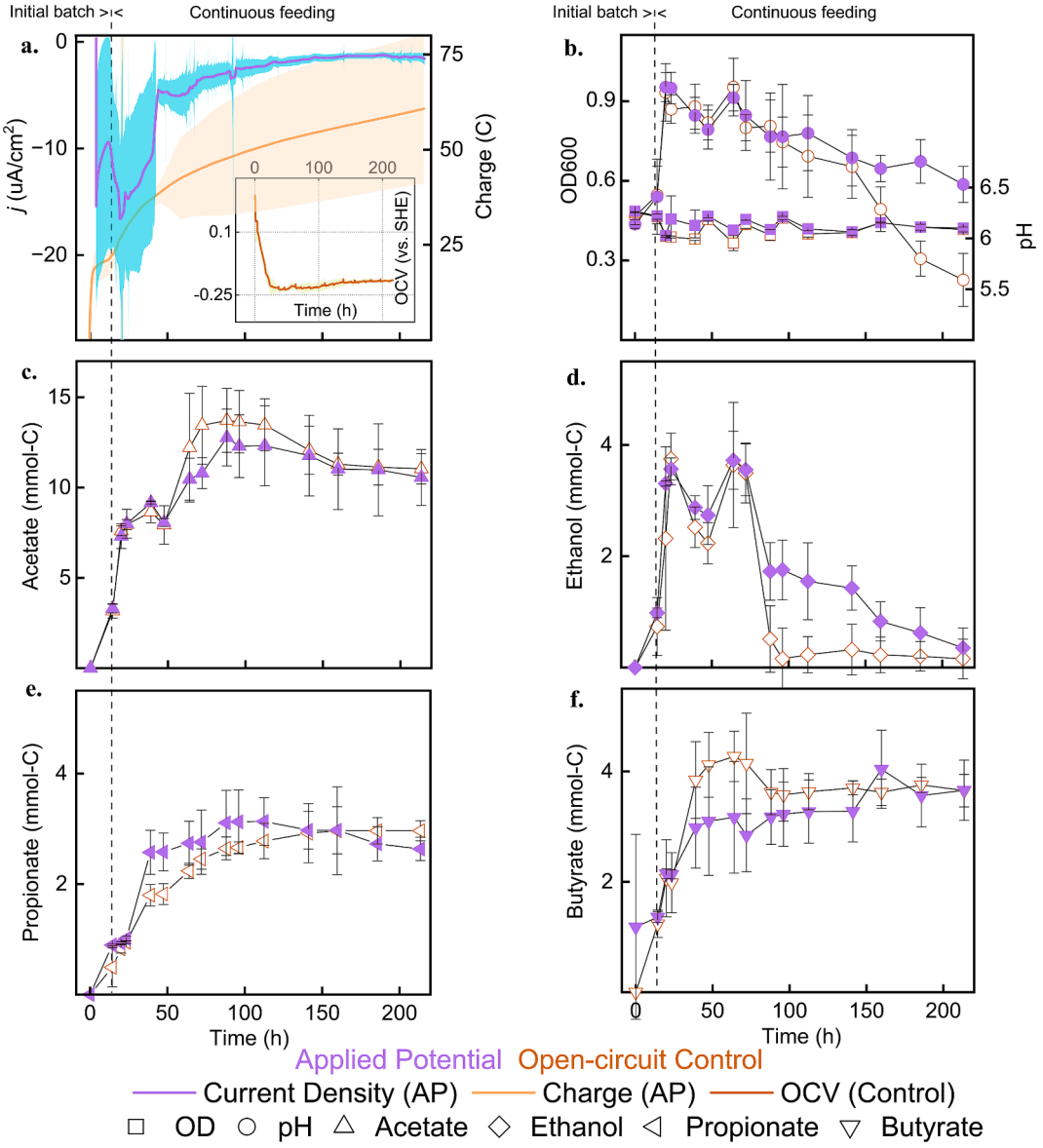

Fig. 2. Mixed culture continuous electro-fermentation using xylose as substrate. Current density, charge logged at a poised cathode potential of −0.40 V, and the recorded open-circuit voltage (a), OD and pH (b), and the accumulated amount of acetate, ethanol, propionate, and butyrate (c-f) measured from the reactor with applied potential (AP) and open-circuit reactors (control). The dashed line denotes when the continuous feeding began. Xylose concentrations can be found in the supplementary file (Fig. S3). All continuous results were based on the average data of three biological replicates, and standard deviations were represented as error bars.

yields remained similar in all the reactors (Fig. S3).

Overall, the repeated batch experiments showed cathode-assisted metabolism towards propionate for 25.6 days, with overall carbon balances of 47 ± 13 % (AP) and 49 ± 5 % (control) and redox balances of 52 ± 15 % (AP) and 53 ± 5 % (control), respectively (Table S3). The observed losses in carbon and redox balances are likely due to the potential growth of planktonic or electrode-attached biomass and any biological gas production during the experiments. Since the cathode potential was fixed at −0.4 V, the electrochemical H_2 production was negligible as suggested from the recorded CV (Fig. S6). Although the batch period showed higher butyrate production in the AP reactors (5.47 ± 0.96 mmol-C, AP vs. 0 mmol-C, control), the long-term repeated batch EF system had limited influence on steering the butyrate production, which may have been related to issues caused by repeated batch configuration, e.g., pH fluctuation, unsolicited biofilm growth, and product inhibition (Jiang et al., 2020). For example, manual pH adjustment in this study offered limited pH control and the pH fluctuated between 5.4 and 6.4. Therefore, continuous systems, which ensure steady-state operation with consistent product yields and minimize fluctuations in environmental conditions, were further tested to fully explore the potential of cathode-assisted propionate and butyrate production in xylose-fed EF systems.

3.2. Limited cathode-assisted metabolism in continuous feeding system

The continuous experiments (Fig. 2) showed similar planktonic cell growth ($OD_{AP/control}$ = 0.9 ± 0.1) with the identical metabolites (i.e., acetate, ethanol, propionate, and butyrate) as the repeated batch experiments before the continuous feeding started (at 19.9 h). Furthermore, higher magnitude of cathodic current densities (−4.2 μA/cm^2) were observed in the continuous reactors (Fig. 2) compared to the repeated batch reactors (−0.0047 μA/cm^2). After 19.9 h, the continuous feeding started with an HRT of 1.1 days, and the current density fluctuated between −15 to −5 μA/cm^2 in AP reactors. Only propionate production showed a minor increase in cathode-assisted systems from 23.4 to 50.0 h compared to the control (2.57 ± 0.40 mmol-C, AP vs. 1.80 ± 0.19 mmol-C, control, Fig. 2). Other metabolites, including acetate and ethanol, showed no differences between AP and control reactors with no increasing of the accumulated amount during the same period of continuous feeding. The hypothesis was that the initiation of continuous feeding may have disrupted the initially established biofilm on the cathode electrode, potentially leading to the washout of specific bacterial populations that could have steered the metabolism under cathodic potentials. Furthermore, more energy was likely distributed to maintain the biofilm growth during continuous operation instead of product formation (Li et al., 2014; Vassilev et al., 2022). After 50 h, acetate production resumed, while the ethanol production stopped after 75 h towards the endpoint, as it was expected to be further metabolised for cell energy-balancing purposes or due to shifts in the microbial communities. Overall, the continuous experiments showed carbon balances of 57 ± 2 % (AP) and 53 ± 2 % (control) and redox balances of 62 ± 3 % (AP) and 57 ± 2 % (control), respectively. The *t*-test results proved no significant differences between the control and AP reactors during the continuous run (Table S4).

The voltage difference between the two electrodes in the control reactors (OCV recorded) dropped from 0.30 V to −0.20 V over the first 24 h and stabilized at −0.20 V for the duration of the experiments (Fig. 2). Although it was uncertain whether OCV data could accurately reflect the redox potential in the fermentation broth, the OCV measurements may help to explain the similar results observed in this study between the control and AP reactors. Overall, the continuous process showed no clear difference in the metabolites between AP and control reactors. The poised potential at −0.40 V compared to the recorded OCV of −0.20 V in the control reactors might have been still unsatisfactory for the bacteria to maintain the energy balance within the ideal range for enhancing propionate and/or butyrate production (Sauer and Teather, 1987). Alternatively, the lower HRT (1.1 d vs. 7.5 d) with higher xylose loading rate during continuous feeding may have initiated biomass washouts, which likely influenced the growth patterns of the microbial communities. This washout was evidenced by lower planktonic cell densities observed in the continuous reactors compared to the repeated batch reactors.

3.3. Microbial communities

The NMDS analysis showed that repeated batch and continuous systems enriched specific bacterial consortia compared to the original inocula (Fig. 3). Certain genera of the bacterial consortia, for example, *Escherichia/Shigella*, *Bacteroides,* and *Lactococcus* were among the dominant genera in both repeated batch and continuous systems, not in the inocula (Fig. 4). In repeated batch systems, PERMANOVA results showed that the clustering of bacterial communities differed between the early phase and the endpoint in planktonic samples (F = 9.98, *p*-value = 0.0019, Table S5) and was influenced by poised cathodic potential (F = 5.15, *p*-value = 0.0152). The highest relative abundant (RA) species at genus level in all repeated batch reactors (Fig. 4) were *Escherichia/Shigella* (RA = 19 ± 12 %), *Bacteroides* (RA = 15 ± 5 %), unclassified genera within the family of *Enterobacteriaceae* (hereinafter 'unclassified *Enterobacteriaceae*,' RA = 9.5 ± 10.0 %) and *Clostridium* sensu stricto 1 (hereinafter '*Clostridium,*' RA = 8 ± 11 %). In the early planktonic samples (113.5 h), where the significant difference in propionate concentration was detected, the relative abundances showed that the AP reactor predominantly enriched *Clostridium* (RA_{AP} = 27 ± 2 % vs. $RA_{control}$ = 4 ± 2 %), unclassified *Enterobacteriaceae* (RA_{AP} = 23.6 ± 0.4 % vs. $RA_{control}$ = 14 ± 5 %) and *Phascolarctobacterium* (RA_{AP} = 11.9 ± 0.1 % vs. $RA_{control}$ = 0.01 ± 0.01 %). In the repeated batch endpoint samples, the enriched consortia in the planktonic samples shifted to *Escherichia/Shigella* (RA_{AP} = 26.7 ± 0.1 % vs. $RA_{control}$ = 32 ± 5 %) and *Bacteroides* (RA_{AP} = 23.6 ± 0.1 % vs. $RA_{control}$ = 14 ± 1 %) dominance in all reactors. Some studies have suggested that *Clostridiaceae* families were accountable for butyrate, acetate, and ethanol production in batch-operated CEF systems when fermenting glucose (Toledo-Alarcón et al., 2019). Given that *Clostridium* genera encompassed several known electroactive bacteria including *Clostridium cochlearium*, *Clostridium pasteurianum* and *Clostridium propionicum* (Choi et al., 2014; Schwab et al., 2019; Zhu et al., 2011), in our repeated batch reactors, the *Clostridium* genera were likely linked to the cathode-assisted propionate and/or butyrate production, the amounts of which were much higher in cathode-enhanced systems during the early stages of the repeated batch reactors compared to the endpoint. However, the link between the substantial decrease in the relative abundance of the *Clostridium* in the planktonic samples and the cathode-assisted propionate and butyrate production after long-term repeated batch operation is still missing.

In continuous experiments, the clustering of bacterial communities was influenced by poised cathodic potential (F = 2.87, *p*-value = 0.0107) but not by the planktonic and biofilm samples (F = 1.59, *p*-value = 0.1433). The most abundant genera in continuous experiments included *Lactococcus* (RA = 14 ± 9 %), *Escherichia/Shigella* (RA = 12 ± 9 %), *Bacteroides* (RA = 7 ± 2 %), and *Fusobacterium* (RA = 7 ± 4 %). Compared to the repeated batch, *Lactococcus* appeared in continuous reactors with higher relative abundances in both planktonic and biofilm samples taken in the control reactors than the AP (RA_{AP} = 10 ± 8 % vs. $RA_{control}$ = 18 ± 8 %). The continuous AP reactors had higher percentages of *Escherichia/Shigella* than the controls in both planktonic and biofilm samples ($RA_{AP,\ planktonic}$ = 23 ± 5 % vs. $RA_{control,\ planktonic}$ = 9 ± 9 % and $RA_{AP,\ biofilm}$ = 11 ± 2 % vs. $RA_{control,\ biofilm}$ = 5 ± 5 %). Many have shown species within *Escherichia/Shigella* and *Lactococcus* to have exoelectrogenic activities in EF systems through metabolic engineering or with added redox mediators (Asefi et al., 2019; Gu et al., 2023, p. 20; Liu et al., 2018). In this study, the functional role of *Escherichia/Shigella* and *Lactococcus* remained unclear.

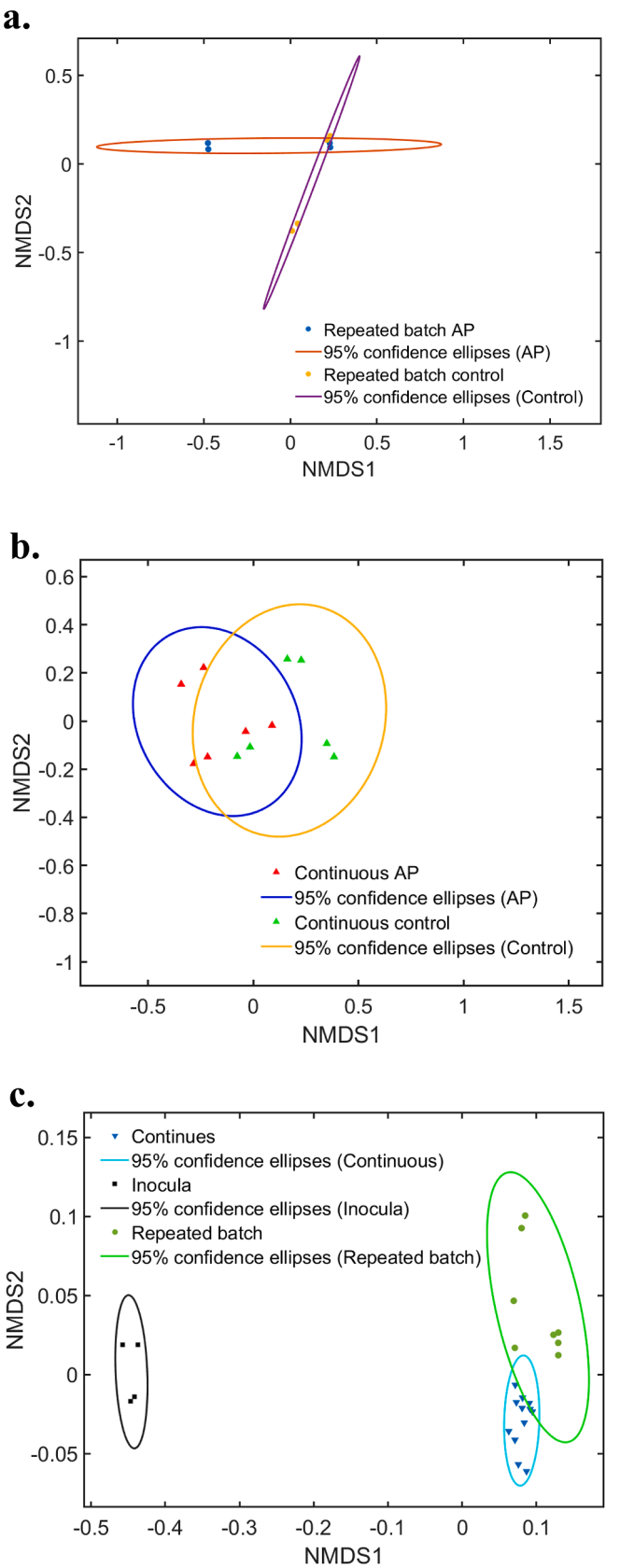

Fig. 3. NMDS analysis of microbial community composition with 95% confidence ellipses for repeated batch (a), continuous (b), and all collected samples compared to inocula (c). The respective PERMANOVA test results on the bacterial community variations for repeated batch, continuous, and all experiments are presented in Table S5.

The PERMANOVA analysis showed statistically significant differences between microbial community samples from repeated batch and continuous systems (F = 8.65, *p*-value = 0.0001, pairwise test *p*-value = 0.003). Meanwhile, the absence of *Clostridium* in endpoint biofilm samples of the AP and control reactors in the continuous systems indicated that biofilm growth with potential CEF activities was not promoted. Nevertheless, it was possible that the species presented with high relative abundance in the microbial communities were not the most active, as the 16S rRNA gene sequencing only revealed the presence of the species and not their activities. Further studies employing metatranscriptomic techniques are essential to identify and characterize the active bacterial species and their functions within the microbial communities.

3.4. Comparing repeated batch to continuous feeding for xylose-based CEF

This study reported, for the first time, propionate and butyrate yields of 0.09 ± 0.05 $mol_{product}/mol_{xylose}$ and 0.09 ± 0.03 $mol_{product}/mol_{xylose}$ from xylose in repeated batch CEF systems with an applied potential of −0.40 V. Higher biomass growth is often measured in the repeated batch fermentation systems compared to systems operated in batch or continuous mode (Yang and Sha, 2019). In this study, the repeated batch system demonstrated a positive correlation between the poised cathodic potential and the growth of propionate-producing biomass. On the other hand, butyrate production in mixed-culture EF systems has been only reported in batch-operated reactors (Toledo-Alarcón et al., 2019). Furthermore, butyrate yield of ca. 0.49 $mol_{product}/mol_{glucose}$ was reported in mixed culture glucose-fed CEF utilizing anthraquinones-2,6-disulphonic salt (AQDS) as mediator and where glucose was fed to the system (Paiano et al. 2019). Our results suggested that the CEF affected butyrate production less during the repeated batch period (41 to 641.5 h) than during the initial batch period (0 to 41 h) and the controls in the same reactors. This study observed noticeable microbial community changes related to *Clostridium* genera in planktonic samples during the 22-day run in repeated batch systems. More fundamental studies of biofilm activities under repeated batch operation and strategies to maintain the desired microbial community (e.g., responsible for propionate or butyrate formation) without excessive biomass washouts are required.

The continuous cathode-assisted EF systems lacked selection pressure for the formation of cathodic biofilm that could steer the metabolite formation. Unlike in the microbial electrosynthesis systems, in which cathodic hydrogen and/or electron production occurs and enhances, e.g., hydrogenotrophic cathodic biofilm formation, the cathode-assisted EF systems are designed mainly for redox-controlling purposes of the fermentation broth (Vassilev et al., 2022; Virdis et al., 2022). The poised cathode potential at −0.40 V did not reach the electrochemical threshold for hydrogen evolution reaction (Fig. S6). Compared to the OCV recorded (−0.20 V) in the fermentation broth of the control reactor, the poised cathode potential may have ineffectively controlled the redox potential on the cellular level during the short HRT. Both the continuous and repeated batch systems showed minimal average current densities (−4.2 μA/cm^2, continuous vs. −0.0047 μA/cm^2, repeated batch), which implied that neither hydrogen was produced nor did the direct electron transfer from the electrode take place. Furthermore, in this study, the continuous process with shorter HRT (1.1 d, continuous vs. 7.5 d, repeated batch) may have required more rapid growth of resilient cathodic biofilm to respond to the biomass washout (Vassilev et al., 2022). Additionally, the 16S rRNA gene results confirmed that the continuous process exhibited lower efficacy in promoting the species that would hypothetically benefit from the cathodic current, and the predominant bacterial genera essential for the EF process, such as the *Clostridium* genera, appeared with low relative abundance under the continuous operation.

Overall, the repeated batch systems showed higher enhanced

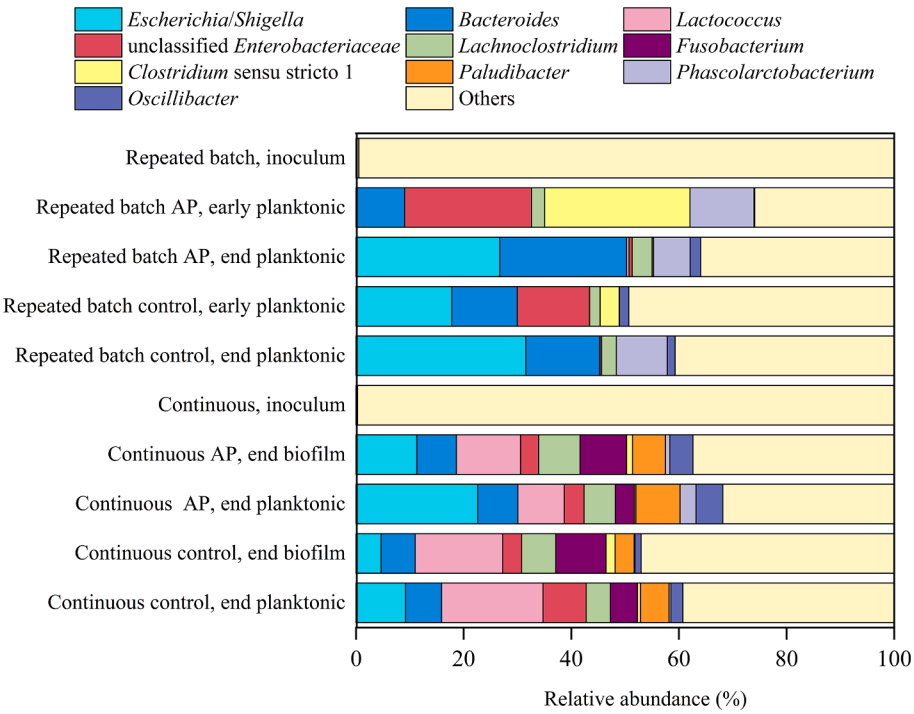

Fig. 4. Ten most abundant genera of inocula and collected planktonic samples at the early phase (113.5 h) and the endpoint (641.5 h) from repeated batch (planktonic samples) and planktonic and biofilm samples at the endpoint (213.5 h) from continuous reactors. All results were based on averaged data of two (repeated batch experiments) and three (continuous experiments) replicates.

propionate and butyrate production rates and yields than the continuous system in the cathode-assisted xylose EF systems. This, linked to the very low current density flowing in the repeated batch systems, makes the EF technology a promising approach to steer fermentation processes towards the production of fermented mixtures with an appropriate ratio between acids with odd and even numbers of carbon atoms, for example to produce biopolymers such as polyhydroxyalkanoates (PHAs) with desired monomeric composition (Bravo-Porras et al., 2024; Carvalheira et al., 2022; Chandra et al., 2023; Dionisi et al., 2004). From the industrial perspective, continuous fermentation systems have been considered economically less competitive than batch and fed-batch systems due to the difficulty of reaching a steady state with mixed culture systems (Yang and Sha, 2019). However, the repeated batch reactors require high-frequency manual operations with careful controls, as different biofilm growth associated with different intercellular redox levels can be triggered by environmental conditions (e.g., oxygen intrusion and phase contaminations) that may further interfere with the EF results (Sun et al., 2023; Vassilev et al., 2022). On the other hand, the continuous system has shown its potential when applying the right selection pressure to closely control the cathodic biofilm's growth in microbial electrosynthesis systems (Vassilev et al., 2022). Future strategies for continuous CEF have to consider biomass immobilization methods (e.g., via change of cathode materials), increasing selection pressure for cathodic biofilm by unlocking potential electron transfer routes (e.g., the addition of redox mediators or introducing genetic engineering tools), and optimizing operation parameters based on the carbon flows and metagenomic analysis.

4. Conclusions

This study investigated the use of xylose as a substrate in mixed culture CEF, comparing repeated batch and continuous feeding strategies to enhance propionate and butyrate production. The repeated batch system demonstrated a simultaneous metabolic shift towards propionate, achieving an overall propionate production rate of 4.4 ± 0.4 mg/L/h (vs. 1.8 ± 0.1 mg/L/h, control) and an overall propionate yield of 0.09 ± 0.05 $mol_{product}/mol_{xylose}$ (vs. 0.06 ± 0.01 $mol_{product}/mol_{xylose}$, control). In contrast, the continuous CEF exhibited more negative current densities (−4.2 μA/cm^2, continuous vs. −0.0047 μA/cm^2 repeated batch) and limited cathode-assisted metabolic activities towards propionate and butyrate production, with an overall propionate yield of 0.06 ± 0.01 $mol_{product}/mol_{xylose}$ (vs. 0.05 ± 0.01 $mol_{product}/mol_{xylose}$, control). Microbial community analysis revealed notable shifts in the abundance of *Clostridium* genera in planktonic samples, particularly in the repeated batch system. Overall, the repeated batch configuration outperformed the continuous system in terms of cathode-assisted propionate and butyrate production, highlighting its potential for optimising cathodic electro-fermentation for sustainable biofuel and biochemical production.

CRediT authorship contribution statement

Yu Sun: Writing – original draft, Visualization, Methodology, Investigation, Funding acquisition, Conceptualization. **Antti J. Rissanen:** Writing – review & editing, Writing – original draft, Visualization, Methodology, Investigation, Conceptualization. **Gaia Salvatori:** Writing – review & editing, Writing – original draft. **Marianna Villano:** Writing – review & editing, Writing – original draft. **Marika Kokko:** Writing – review & editing, Writing – original draft, Supervision, Methodology, Investigation, Funding acquisition, Conceptualization.

Declaration of competing interest

The authors declare that they have no known competing financial interests or personal relationships that could have appeared to influence the work reported in this paper.

Acknowledgments

Y.S. acknowledges the financial support from the Finnish Foundation

for Technology Promotion (Grant No. 10026) and the Tampere University Doctoral School. The authors would also like to thank Mika Karttunen for invaluable laboratory support and assistance in collecting municipal sewage sludge.

Appendix A. Supplementary data

Supplementary data to this article can be found online at https://doi.org/10.1016/j.biortech.2025.132787.

Data availability

Data will be made available on request.

References

Anderson, M.J., 2017. Permutational Multivariate Analysis of Variance (PERMANOVA). In: Wiley StatsRef: Statistics Reference Online. John Wiley & Sons Ltd, pp. 1–15. https://doi.org/10.1002/9781118445112.stat07841.

Asefi, B., Li, S.-L., Moreno, H.A., Sanchez-Torres, V., Hu, A., Li, J., Yu, C.-P., 2019. Characterization of electricity production and microbial community of food waste-fed microbial fuel cells. Process Saf. Environ. Prot. 125, 83–91. https://doi.org/10.1016/j.psep.2019.03.016.

Bolger, A.M., Lohse, M., Usadel, B., 2014. Trimmomatic: a flexible trimmer for Illumina sequence data. Bioinformatics 30, 2114–2120. https://doi.org/10.1093/bioinformatics/btu170.

Bolyen, E., Rideout, J.R., Dillon, M.R., Bokulich, N.A., Abnet, C.C., Al-Ghalith, G.A., Alexander, H., Alm, E.J., Arumugam, M., Asnicar, F., Bai, Y., Bisanz, J.E., Bittinger, K., Brejnrod, A., Brislawn, C.J., Brown, C.T., Callahan, B.J., Caraballo-Rodríguez, A.M., Chase, J., Cope, E.K., Da Silva, R., Diener, C., Dorrestein, P.C., Douglas, G.M., Durall, D.M., Duvallet, C., Edwardson, C.F., Ernst, M., Estaki, M., Fouquier, J., Gauglitz, J.M., Gibbons, S.M., Gibson, D.L., Gonzalez, A., Gorlick, K., Guo, J., Hillmann, B., Holmes, S., Holste, H., Huttenhower, C., Huttley, G.A., Janssen, S., Jarmusch, A.K., Jiang, L., Kaehler, B.D., Kang, K.B., Keefe, C.R., Keim, P., Kelley, S.T., Knights, D., Koester, I., Kosciolek, T., Kreps, J., Langille, M.G.I., Lee, J., Ley, R., Liu, Y.-X., Loftfield, E., Lozupone, C., Maher, M., Marotz, C., Martin, B.D., McDonald, D., McIver, L.J., Melnik, A.V., Metcalf, J.L., Morgan, S.C., Morton, J.T., Naimey, A.T., Navas-Molina, J.A., Nothias, L.F., Orchanian, S.B., Pearson, T., Peoples, S.L., Petras, D., Preuss, M.L., Pruesse, E., Rasmussen, L.B., Rivers, A., Robeson, M.S., Rosenthal, P., Segata, N., Shaffer, M., Shiffer, A., Sinha, R., Song, S.J., Spear, J.R., Swafford, A.D., Thompson, L.R., Torres, P.J., Trinh, P., Tripathi, A., Turnbaugh, P.J., Ul-Hasan, S., van der Hooft, J.J.J., Vargas, F., Vázquez-Baeza, Y., Vogtmann, E., von Hippel, M., Walters, W., Wan, Y., Wang, M., Warren, J., Weber, K.C., Williamson, C.H.D., Willis, A.D., Xu, Z.Z., Zaneveld, J.R., Zhang, Y., Zhu, Q., Knight, R., Caporaso, J.G., 2019. Reproducible, interactive, scalable and extensible microbiome data science using QIIME 2. Nat. Biotechnol. 37, 852–857. https://doi.org/10.1038/s41587-019-0209-9.

Bravo-Porras, G., Fernández-Güelfo, L.A., Álvarez-Gallego, C.J., Carbú, M., Sales, D., Romero-García, L.I., 2024. Influence of the total concentration and the profile of volatile fatty acids on polyhydroxyalkanoates (PHA) production by mixed microbial cultures. Biomass Conv. Bioref. 14, 239–253. https://doi.org/10.1007/s13399-021-02208-z.

Callahan, B.J., McMurdie, P.J., Rosen, M.J., Han, A.W., Johnson, A.J.A., Holmes, S.P., 2016. DADA2: High-resolution sample inference from Illumina amplicon data. Nat. Methods 13, 581–583. https://doi.org/10.1038/nmeth.3869.

Carvalheira, M., Hilliou, L., Oliveira, C.S.S., Guarda, E.C., Reis, M.A.M., 2022. Polyhydroxyalkanoates from industrial cheese whey: production and characterization of polymers with differing hydroxyvalerate content. Curr. Res. Biotechnol. 4, 211–220. https://doi.org/10.1016/j.crbiot.2022.03.004.

Chandra, R., Thakor, A., Mekonnen, T.H., Charles, T.C., Lee, H.-S., 2023. Production of polyhydroxyalkanoate (PHA) copolymer from food waste using mixed culture for carboxylate production and Pseudomonas putida for PHA synthesis. J. Environ. Manage. 336, 117650. https://doi.org/10.1016/j.jenvman.2023.117650.

Choi, O., Kim, T., Woo, H.M., Um, Y., 2014. Electricity-driven metabolic shift through direct electron uptake by electroactive heterotroph Clostridiumpasteurianum. Sci. Rep. 4, 6961. https://doi.org/10.1038/srep06961.

Cinar, A., Parulekar, S.J., Undey, C., Birol, G., 2003. Batch fermentation: modeling: monitoring, and control. CRC Press, New York. https://doi.org/10.1201/9780203911358.

Cirino, P.C., Chin, J.W., Ingram, L.O., 2006. Engineering Escherichia coli for xylitol production from glucose-xylose mixtures. Biotechnol. Bioeng. 95, 1167–1176. https://doi.org/10.1002/bit.21082.

Dai, K., Wen, J.-L., Zhang, F., Zeng, R.J., 2017. Valuable biochemical production in mixed culture fermentation: fundamentals and process coupling. Appl. Microbiol. Biotechnol. 101, 6575–6586. https://doi.org/10.1007/s00253-017-8441-z.

Demirbas, A., 2011. Waste management, waste resource facilities and waste conversion processes. Energ. Conver. Manage. 52, 1280–1287. https://doi.org/10.1016/j.enconman.2010.09.025.

Dionisi, D., Majone, M., Papa, V., Beccari, M., 2004. Biodegradable polymers from organic acids by using activated sludge enriched by aerobic periodic feeding. Biotechnol. Bioeng. 85, 569–579. https://doi.org/10.1002/bit.10910.

Domingues, R., Bondar, M., Palolo, I., Queirós, O., de Almeida, C.D., Cesário, M.T., 2021. Xylose Metabolism in Bacteria—opportunities and challenges towards efficient lignocellulosic biomass-based biorefineries. Appl. Sci. 11, 8112. https://doi.org/10.3390/app11178112.

Edgar, R.C., 2010. Search and clustering orders of magnitude faster than BLAST. Bioinformatics 26, 2460–2461. https://doi.org/10.1093/bioinformatics/btq461.

Edgar, R.C., Haas, B.J., Clemente, J.C., Quince, C., Knight, R., 2011. UCHIME improves sensitivity and speed of chimera detection. Bioinformatics 27, 2194–2200. https://doi.org/10.1093/bioinformatics/btr381.

Engel, M., Holtmann, D., Ulber, R., Tippkötter, N., 2019. Increased biobutanol production by mediator-less electro-fermentation. Biotechnol. J. 14. https://doi.org/10.1002/biot.201800514.

Gu, L., Xiao, X., Yup Lee, S., Lai, B., Solem, C., 2023. Superior anodic electro-fermentation by enhancing capacity for extracellular electron transfer. Bioresour. Technol. 389, 129813. https://doi.org/10.1016/j.biortech.2023.129813.

Gu, Y., Ding, Y., Ren, C., Sun, Z., Rodionov, D.A., Zhang, W., Yang, S., Yang, C., Jiang, W., 2010. Reconstruction of xylose utilization pathway and regulons in Firmicutes. BMC Genom. 11, 255. https://doi.org/10.1186/1471-2164-11-255.

Guan, N., Li, J., Shin, H., Du, G., Chen, J., Liu, L., 2017. Microbial response to environmental stresses: from fundamental mechanisms to practical applications. Appl. Microbiol. Biotechnol. 101, 3991–4008. https://doi.org/10.1007/s00253-017-8264-y.

Hammer, Ø., Harper, D.A.T., Ryan, P.D., 2001. PAST: paleontological statistics software package for education and data analysis. Palaeontol. Electron. 4, 9. http://palaeo-electronica.org/2001_1/past/issue1_01.htm.

Jeffries, T.W., 1983. Utilization of xylose by bacteria, yeasts, and fungi. Adv. Biochem. Eng. Biotechnol. 27, 1–32. https://doi.org/10.1007/BFb0009101.

Jiang, Y., Chu, N., Zhang, W., Zhang, L., Jianxiong Zeng, R., 2020. Electro-fermentation regulates mixed culture chain elongation with fresh and acclimated cathode. Energ. Conver. Manage. 204, 112285. https://doi.org/10.1016/j.enconman.2019.112285.

Jiang, Y., Lu, L., Wang, H., Shen, R., Ge, Z., Hou, D., Chen, X., Liang, P., Huang, X., Ren, Z.J., 2018. Electrochemical control of redox potential arrests methanogenesis and regulates products in mixed culture electro-fermentation. ACS Sustainable Chem. Eng. 6, 8650–8658. https://doi.org/10.1021/acssuschemeng.8b00948.

Johnson, A., 2024. error_ellipse [WWW Document]. URL https://se.mathworks.com/matlabcentral/fileexchange/4705-error_ellipse (accessed 11.11.24).

Khedkar, M., Bedade, D., Singhal, R.S., Bankar, S.B., 2024. Mixed Culture Cultivation in Microbial Bioprocesses. Springer, Berlin, Heidelberg, pp. 1–61.

Kongjan, P., Min, B., Angelidaki, I., 2009. Biohydrogen production from xylose at extreme thermophilic temperatures (70 °C) by mixed culture fermentation. Water Res. 43, 1414–1424. https://doi.org/10.1016/j.watres.2008.12.016.

Kracke, F., Krömer, J.O., 2014. Identifying target processes for microbial electrosynthesis by elementary mode analysis. BMC Bioinf. 15, 410. https://doi.org/10.1186/s12859-014-0410-2.

Lee, J., Lee, S.Y., Park, S., Middelberg, A.P.J., 1999. Control of fed-batch fermentations. Biotechnol. Adv. 17, 29–48. https://doi.org/10.1016/S0734-9750(98)00015-9.

Li, T., Chen, X., Chen, J., Wu, Q., Chen, G.-Q., 2014. Open and continuous fermentation: Products, conditions and bioprocess economy. Biotechnol. J. 9, 1503–1511. https://doi.org/10.1002/biot.201400084.

Liu, R., Liang, L., Chen, K., Ma, J., Jiang, M., Wei, P., Ouyang, P., 2012. Fermentation of xylose to succinate by enhancement of ATP supply in metabolically engineered Escherichia coli. Appl. Microbiol. Biotechnol. 94, 959–968. https://doi.org/10.1007/s00253-012-3896-4.

Liu, X., Shi, L., Gu, J.D., 2018. Microbial electrocatalysis: redox mediators responsible for extracellular electron transfer. Biotechnol. Adv. 36, 1815–1827. https://doi.org/10.1016/j.biotechadv.2018.07.001.

Martin, M., 2011. Cutadapt removes adapter sequences from high-throughput sequencing reads. Embnet. J. 17, 10–12. https://doi.org/10.14806/ej.17.1.200.

Martínez-Ruano, J.A., Suazo, A., Véliz, F., Otalora, F., Conejeros, R., González, E., Aroca, G., 2024. Effect of pH on metabolic pathway shift in fermentation and electro-fermentation of xylose by Clostridium autoethanogenum. J. Environ. Manage. 351, 119918. https://doi.org/10.1016/j.jenvman.2023.119918.

Moscoviz, R., Toledo-Alarcón, J., Trably, E., Bernet, N., 2016. Electro-fermentation: how to drive fermentation using electrochemical systems. Trends Biotechnol. 34, 856–865. https://doi.org/10.1016/j.tibtech.2016.04.009.

Moscoviz, R., Trably, E., Bernet, N., Carrère, H., 2018. The environmental biorefinery: state-of-the-art on the production of hydrogen and value-added biomolecules in mixed-culture fermentation. Green Chem. 20, 3159–3179. https://doi.org/10.1039/C8GC00572A.

Nanda, S., Azargohar, R., Dalai, A.K., Kozinski, J.A., 2015. An assessment on the sustainability of lignocellulosic biomass for biorefining. Renew. Sustain. Energy Rev. 50, 925–941. https://doi.org/10.1016/j.rser.2015.05.058.

Octave, S., Thomas, D., 2009. Biorefinery: toward an industrial metabolism. Biochimie, Lipids for the Future 91, 659–664. https://doi.org/10.1016/j.biochi.2009.03.015.

Oksanen, J., Simpson, G.L., Blanchet, F.G., Kindt, R., Legendre, P., Minchin, P.R., O'Hara, R.B., Solymos, P., Stevens, M.H.H., Szoecs, E., Wagner, H., Barbour, M., Bedward, M., Bolker, B., Borcard, D., Carvalho, G., Chirico, M., De Caceres, M., Durand, S., Evangelista, H.B.A., FitzJohn, R., Friendly, M., Furneaux, B., Hannigan, G., Hill, M.O., Lahti, L., McGlinn, D., Ouellette, M.-H., Ribeiro Cunha, E., Smith, T., Stier, A., Ter Braak, C.J.F., Weedon, J., 2001. vegan: Community Ecology Package. doi.org/10.32614/CRAN.package.vegan.

Paiano, P., Menini, M., Zeppilli, M., Majone, M., Villano, M., 2019. Electro-fermentation and redox mediators enhance glucose conversion into butyric acid with mixed microbial cultures. Bioelectrochemistry 130. https://doi.org/10.1016/j.bioelechem.2019.107333.

Ponnusamy, V.K., Nguyen, D.D., Dharmaraja, J., Shobana, S., Banu, J.R., Saratale, R.G., Chang, S.W., Kumar, G., 2019. A review on lignin structure, pretreatments, fermentation reactions and biorefinery potential. Bioresour. Technol. 271, 462–472. https://doi.org/10.1016/j.biortech.2018.09.070.

Qian, D.-K., Geng, Z.-Q., Sun, T., Dai, K., Zhang, W., Jianxiong Zeng, R., Zhang, F., 2020. Caproate production from xylose by mesophilic mixed culture fermentation. Bioresour. Technol. 308, 123318. https://doi.org/10.1016/j.biortech.2020.123318.

Quast, C., Pruesse, E., Yilmaz, P., Gerken, J., Schweer, T., Yarza, P., Peplies, J., Glöckner, F.O., 2013. The SILVA ribosomal RNA gene database project: improved data processing and web-based tools. Nucleic Acids Res. 41, D590–D596. https://doi.org/10.1093/nar/gks1219.

Sauer, F.D., Teather, R.M., 1987. Changes in oxidation reduction potentials and volatile fatty acid production by rumen bacteria when methane synthesis is inhibited1. J. Dairy Sci. 70, 1835–1840. https://doi.org/10.3168/jds.S0022-0302(87)80222-9.

Schievano, A., Sciarria, T.P., Vanbroekhoven, K., Wever, H.D., Puig, S., Andersen, S.J., Rabaey, K., Pant, D., 2016. Electro-fermentation – merging electrochemistry with fermentation in industrial applications. Trends Biotechnol. 34, 866–878. https://doi.org/10.1016/j.tibtech.2016.04.007.

Schwab, L., Rago, L., Koch, C., Harnisch, F., 2019. Identification of Clostridium cochlearium as an electroactive microorganism from the mouse gut microbiome. Bioelectrochemistry 130, 107334. https://doi.org/10.1016/j.bioelechem.2019.107334.

Sun, Y., Kokko, M., Vassilev, I., 2023. Anode-assisted electro-fermentation with Bacillus subtilis under oxygen-limited conditions. Biotechnol. Biofuels 16, 6. https://doi.org/10.1186/s13068-022-02253-4.

Tang, J., Dai, K., Wang, Q.-T., Zheng, S.-J., Hong, S.-D., Jianxiong Zeng, R., Zhang, F., 2022. Caproate production from xylose via the fatty acid biosynthesis pathway by genus *Caproiciproducens* dominated mixed culture fermentation. Bioresour. Technol. 351, 126978. https://doi.org/10.1016/j.biortech.2022.126978.

Temudo, M.F., Mato, T., Kleerebezem, R., van Loosdrecht, M.C.M., 2009. Xylose anaerobic conversion by open-mixed cultures. Appl. Microbiol. Biotechnol. 82, 231–239. https://doi.org/10.1007/s00253-008-1749-y.

Toledo-Alarcón, J., Moscoviz, R., Trably, E., Bernet, N., 2019. Glucose electro-fermentation as main driver for efficient H2-producing bacteria selection in mixed cultures. Int. J. Hydrogen Energy 44, 2230–2238. https://doi.org/10.1016/j.ijhydene.2018.07.091.

Trchounian, A., Trchounian, K., 2019. Fermentation revisited: how do microorganisms survive under energy-limited conditions? Trends Biochem. Sci 44, 391–400. https://doi.org/10.1016/j.tibs.2018.12.009.

UN, 2021. Food and Agriculture Organization of the United Nations [WWW Document]. URL https://www.fao.org/faostat/en/?#data/GT (accessed 11.11.24).

Vassilev, I., Averesch, N.J.H., Ledezma, P., Kokko, M., 2021. Anodic electro-fermentation: empowering anaerobic production processes via anodic respiration. Biotechnol. Adv. 48, 107728. https://doi.org/10.1016/j.biotechadv.2021.107728.

Vassilev, I., Dessì, P., Puig, S., Kokko, M., 2022. Cathodic biofilms – a prerequisite for microbial electrosynthesis. Bioresour. Technol. 348, 126788. https://doi.org/10.1016/j.biortech.2022.126788.

Virdis, B., Hoelzle, D.R., Marchetti, A., Boto, S.T., Rosenbaum, M.A., Blasco-Gómez, R., Puig, S., Freguia, S., Villano, M., 2022. Electro-fermentation: sustainable bioproductions steered by electricity. Biotechnol. Adv. 59, 107950. https://doi.org/10.1016/j.biotechadv.2022.107950.

Yang, Y., Sha, M., 2019. A beginner's guide to bioprocess modes – batch, fed- batch, and continuous fermentation. Enfield, CT 1–16.

Zhang, B., Zhang, J., Wang, D., Han, R., Ding, R., Gao, X., Sun, L., Hong, J., 2016a. Simultaneous fermentation of glucose and xylose at elevated temperatures co-produces ethanol and xylitol through overexpression of a xylose-specific transporter in engineered *Kluyveromyces marxianus*. Bioresour. Technol. 216, 227–237. https://doi.org/10.1016/j.biortech.2016.05.068.

Zhang, F., Li, J., Liu, H., Liang, Q., Qi, Q., 2016b. ATP-based ratio regulation of glucose and xylose improved succinate production. PLOS ONE 11, e0157775. https://doi.org/10.1371/journal.pone.0157775.

Zhao, Z., Xian, M., Liu, M., Zhao, G., 2020. Biochemical routes for uptake and conversion of xylose by microorganisms. Biotechnol. Biofuels 13, 21. https://doi.org/10.1186/s13068-020-1662-x.

Zhu, L., Chen, H., Huang, L., Cai, J., Xu, Z., 2011. Electrochemical analysis of Clostridium propionicum and its acrylic acid production in microbial fuel cells. Eng. Life Sci. 11, 238–244. https://doi.org/10.1002/elsc.201000220.